

# Experimentally-based Viscoelastic Model for Polyurea, Including Pressure and Temperature Effects

Alireza V. Amirkhizi, Graduate Student, Center of Excellence for Advanced Materials, Department of Mechanical and Aerospace Engineering, University of California, San Diego, La Jolla, CA 92093-0416

Jon Isaacs, Sr. Development Engineer, Center of Excellence for Advanced Materials, Department of Mechanical and Aerospace Engineering, University of California, San Diego, La Jolla, CA 92093-0416

Sia Nemat-Nasser, Professor, Center of Excellence for Advanced Materials, Department of Mechanical and Aerospace Engineering, University of California, San Diego, La Jolla, CA 92093-0416

## ABSTRACT

The results of a systematic study of the viscoelastic properties of polyurea over broad ranges of strain rates, temperatures, and pressures are presented. Based on the experimental data and a master curve developed by Knauss [1] we have produced a model for large-deformation viscoelastic response of this elastomer. High strain-rate data are obtained using Hopkinson bar experiments. We show that the inclusion of pressure sensitivity into the model successfully reproduces the experimental results. We also present an equivalent simplified model that involves a finite number of internal state variables tailored for implementation into explicit finite-element codes. The model incorporates the classical Williams-Landel-Ferry (WLF) time-temperature transformation [2] and pressure sensitivity, in addition to a thermodynamically sound dissipation mechanism. Finally we show that using this model for the shear behavior of polyurea along with the elastic bulk response, one can successfully reproduce the very high strain rate pressure-shear experimental results recently reported by Clifton and Jiao [3].

## Constitutive model

We have developed a complete model for the response of polyurea under a wide range of strain-rate, temperature, and pressure. Most polymers have substantially different behavior under shearing and volumetric deformations. In this case, shear deformation is modeled by a temperature- and pressure-dependent viscoelastic relaxation modulus. The volumetric response is also temperature-sensitive but is modeled as nonlinearly elastic. Here we summarize this model; for more detail see [4].

Based on WLF time-temperature superposition principle, the shear relaxation curve of a polymer can be represented for any temperature in the range  $T_g < T < T_g + 100K$ , as,

$$G(t, T) = \frac{T}{T_{ref}} G\left(\frac{t}{a(T, P)}, T_{ref}\right). \quad (1)$$

Here  $T_g$  is the glass transition temperature,  $G(t, T)$  is the relaxation modulus at temperature  $T$ ,  $T_{ref}$  is a reference temperature usually taken to be  $T_g + 50K$ , and  $a(T, P)$  is the ratio of the relaxation time-scale at temperature  $T$  and pressure  $P$  to that at the *reference conditions*,  $T_{ref}$  and zero pressure:

$T_{ref}(K)$	$A$	$B(K)$	$C_p(K/GPa)$	$C_V(J/mm^3/K)$	$CTE(/K)$	$m(GPa/K)$	$n$	$\kappa_{ref}(GPa)$	$G_\infty(GPa)$
273	-10	107.54	7.2	$1.977 \times 10^{-3}$	$2 \times 10^{-4}$	-0.015	4	4.948	0.0224
$p_1$	$p_2$	$p_3$	$p_4$	$q_1(ms)$	$q_2(ms)$	$q_3(ms)$	$q_4(ms)$		
0.8458	1.686	3.594	4.342	463.4	0.06407	$1.163 \times 10^{-4}$	$7.321 \times 10^{-7}$		

**Table 1.** Constitutive parameters of polyurea used in numerical modeling. All parameters except for the heat capacity  $C_V$  and the coefficient of thermal expansion  $CTE$  are defined in the text.

$$a(T, P) = a(T') = \frac{\tau(T')}{\tau_{ref}} = 10^{\frac{A(T'-T_{ref})}{B+T'-T_{ref}}} \quad (2)$$

Here  $A$  and  $B$  are material properties, and  $T'$  is the effective temperature that depends linearly on pressure,  $T' = T - C_p P$ . (3)

The master curve can be approximated by a Prony series with any number of terms,

$$G_{ref}(t) = G_\infty \left( 1 + \sum_{i=1}^n p_i e^{-t/q_i} \right) \quad (4)$$

The time integrals needed for the stress calculation can then be evaluated at each time step using a finite number of appropriate internal state variables. Otherwise, one would need to integrate the complete deformation history at each time step increment, which would render numerical calculations prohibitively resource consuming. Furthermore the dissipated power is also calculated using the same state variables,

$$\frac{\partial W_d}{\partial t} = G_\infty \frac{T(t)}{T_{ref}} \sum_{i=1}^n \frac{p_i}{q_i} \boldsymbol{\varepsilon}_d^i(t) : \boldsymbol{\varepsilon}_d^i(t), \quad (5)$$

Here  $W_d$  is the dissipated work and  $\boldsymbol{\varepsilon}_d^i(t)$  is the  $i$ -th internal variable. The pressure is calculated from the volumetric deformation,

$$P = -\kappa \frac{\ln J}{J}, \quad (6)$$

where  $J$  is the Jacobian of the deformation, and  $\kappa$  is a temperature dependent bulk modulus,

$$\kappa(T) = \kappa(T_{ref}) + m(T - T_{ref}). \quad (7)$$

### Split Hopkinson-bar experiments

We have performed a series of split-Hopkinson bar experiments on polyurea under various conditions. To verify the model discussed above, a selected set of these experiments is used here. The tests presented here were all performed at an effective engineering strain rate of  $3000 \pm 400/s$ . The summary of the experimental parameters is given in Table 2. All 4 tests are performed using a 12.7mm split-Hopkinson bar (maraging steel bars). For the confined tests, the sample is fitted inside a steel cylindrical tube of 17.8mm OD and 26mm length. The Cauchy stress must be estimated for the unconfined test since the diameter of the sample changes with increasing axial load. Since under the low pressures observed in the unconfined tests, polyurea is nearly incompressible, we calculated the diameter and the Cauchy stress assuming isochoric deformation. The resulting loading stress-strain curves are shown in Figure 1. From the initial part of the unloading curves, one observes that, for the confined tests, the unloading follows essentially the same stress-strain path as that of the loading. In the unconfined case, however, the stress is released faster than the accumulated strain. This strain is not permanent though and, in all cases, the sample regained its initial length after the test was completed.

### FEM modeling of a pressure-shear test

The constitutive model has been used to simulate one of the pressure-shear tests performed at Brown University and documented in [3]. A steel flyer plate ( $T_{flyer} = 6.991mm$ ) impacts at velocity  $V_0 = 112.6m/s$  a sandwich structure that consists of a front steel plate ( $T_{front} = 2.896mm$ ), a thin layer of elastomer ( $T_{elastomer} = 0.11mm$ ), and a rear steel

plate ( $T_{rear} = 7.041\text{mm}$ ). All of the plates are aligned at a  $\theta = 18^\circ$  angle with respect to the velocity direction and have diameter  $D = 60\text{mm}$ ; see Figure 2. Upon impact, elastic waves are created that travel normal to the surface of the impact. These are: a longitudinal compression wave (high velocity) and a shear wave (low velocity). The impact parameters are set such that the steel plates remain elastic. The longitudinal pressure wave reaches the elastomer layer first and loads it to a maximum stress after a few reverberations. Both normal and transverse particle velocities are measured on the back surface of the rear plate using optical methods.

Name	Confinement	Diameter (mm)	Length(mm)	Effective Strain Rate (/s)	Temperature (K)
UC	No	6.17	1.78	3400	294
CL	Yes	12.7	5.08	2600	273
CR	Yes	12.7	5.08	2800	294
CH	Yes	12.7	5.08	2800	333

**Table 2.** Hopkinson-bar experiments setup.

The center of the whole structure, consisting of the flyer, front, and rear plates and the elastomer layer is modeled with three-dimensional elements using the elastic properties of steel and the nonlinear viscoelastic user-defined constitutive subroutine for the polyurea. The boundary conditions are prescribed such that the material is confined laterally but allow for shear deformation. We constrained the top and bottom nodes to have the same displacement degrees of freedom; see Figure 2. This maintains a fixed lateral dimension and hence the confining pressure is applied automatically by the finite-element solver. At the same time the element can be sheared laterally.

The propagation of a finite amplitude elastic shear wave in a uniaxially pre-strained layer of elastomer has been discussed in [5]. The expected particle velocity on the back surface of the rear plate for an elastic wave would consist of stepped rises that finally converge to the impact transverse velocity regardless of the stiffness of the elastomer; see Figure 3. Neither of these two properties is observed in the measured transverse velocity by Clifton and Jiao [3]. Instead, there is a single jump at the beginning, followed by a gradual rise in the velocity. We sought to reproduce these characteristics using our viscoelastic model. The parameters are as listed in Table 1 except for the ones indicated in the graph and a linear bulk modulus of elasticity of  $\kappa = 22.5\text{GPa}$ . The long-time shear modulus,  $G_\infty$ , and the pressure-sensitivity parameter,  $C_{ip}$ , are modified to examine their effects. Since we are primarily interested in the shear behavior of the elastomer under stress, a linearly elastic model is used for the bulk response to simplify the calculation. Figure 3 shows that the viscoelastic model properly captures the qualitative behavior seen in the experiment. By changing the long-time shear modulus and the pressure-sensitivity parameter we are able to reproduce the experimental data with reasonable accuracy.

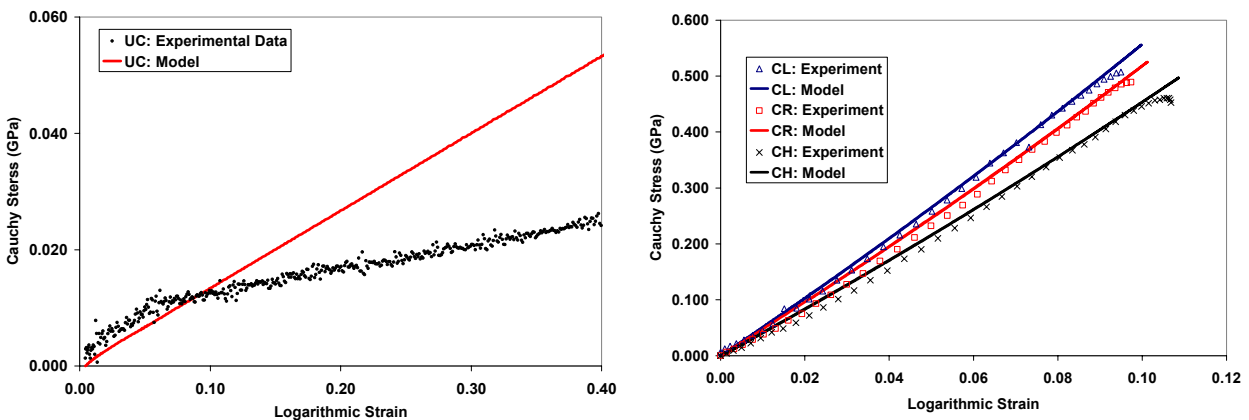


**Figure 1.** [Left] The unconfined Hopkinson-bar test results for polyurea at  $T=273\text{K}$ , and the constitutive-model result, valid up to 8% strain; the stress is estimated based on the lateral expansion predicted by the model. [Right] Confined Hopkinson-bar test and the constitutive-model results.

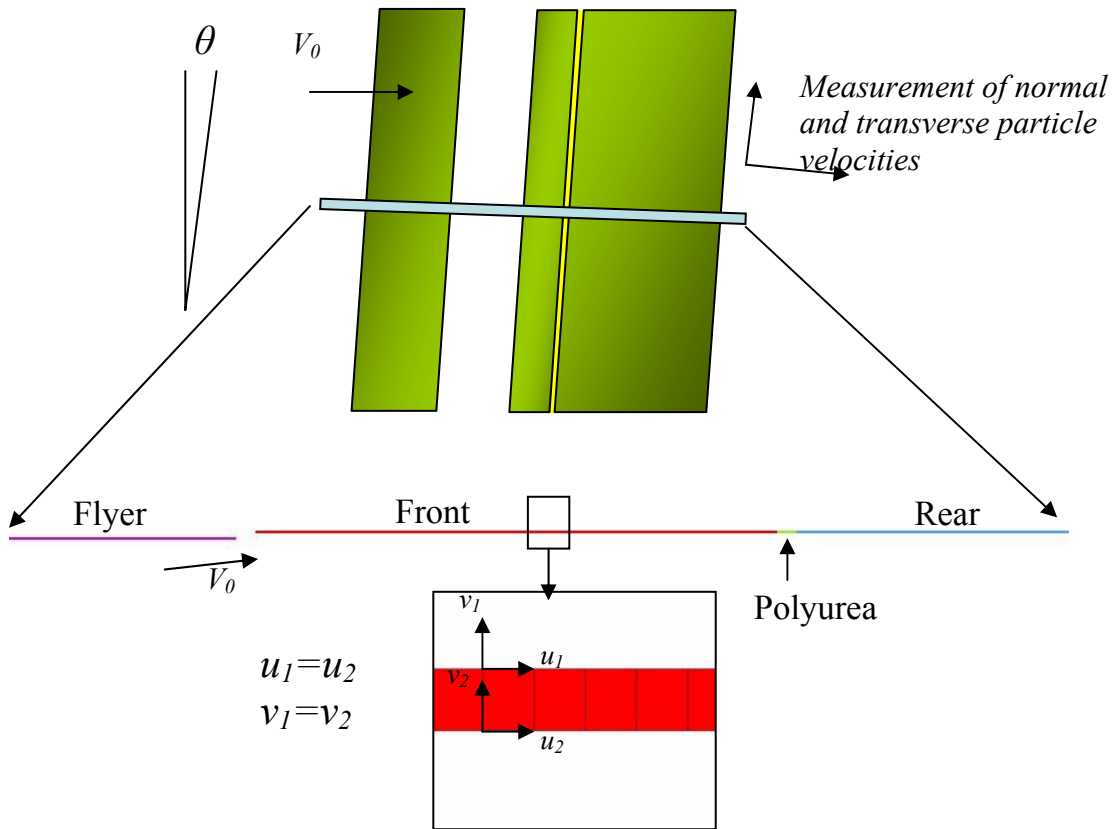


**Figure 2.** Schematics of the pressure–shear experiment and the FEM model. [Top] Flyer plate impacts the front plate at velocity  $V_0$ , creating normal and transverse elastic waves that travel and load the polyurea layer and eventually the back plate. [Middle] The elements along the center line passing through the plates and polyurea layer are modeled using LS-DYNA [6]. [Bottom] The constrained central elements.

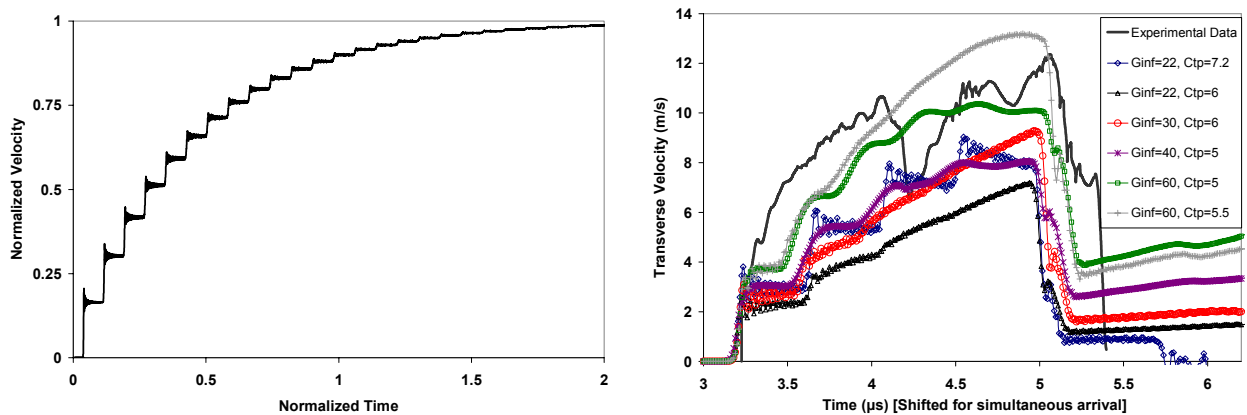


**Figure 3.** [Left] The profile of the normalized transverse particle velocity (divided by  $V_0 \sin\theta$ ) on the back surface of the rear plate for a fully elastic material. The time is normalized through dividing by  $(l/(V_0 \sin\theta))$ , where  $l$  is the thickness of the elastomer. [Right] The profile of the transverse particle velocity as measured and calculated on the back surface of the rear plate. The solid curve depicts the experimental results [3] and other curves show the various possible responses by varying two parameters: the equilibrium shear modulus,  $G_\infty$  (in MPa), and the pressure-sensitivity parameter,  $C_{tp}$  (in K/GPa).

## Acknowledgements

The authors wish to thank Rod Clifton and Tong Jiao for sharing with us the data from their pressure-shear experiments and Wolfgang Knauss for providing us with the relaxation master curve of polyurea. This work was supported by ONR N00014-03-M-0172 under Dr. Roshdy Barsoum's program.

## References

- [1] Knauss, W. "Viscoelastic material characterization relative to constitutive and failure response of an elastomer" *Interim Report to the Office of Naval Research*, GALCIT, Pasadena, CA, 2003.
- [2] Williams, M. L., Landel, R. F., Ferry, J. D., "The Temperature Dependence of Relaxation Mechanisms in Amorphous Polymers and Other Glass-forming Liquids" *J. Am. Chem. Soc.*, Vol. 77, 3701-7, 1955.
- [3] Clifton, R., Jiao, T. "High strain rate response of elastomers" in: *Presentation to ERC ACTD Workshop*, Cambridge, MA, 2004.
- [4] Amirkhizi, A. V., Isaacs, J., McGee, J., and Nemat-Nasser, S. "An experimentally-based viscoelastic constitutive model for polyurea, including pressure and temperature effects" submitted to *Philosophical Magazine*, 2006 (in review).
- [5] Nemat-Nasser S., Amirkhizi, A. V. "Finite amplitude shear wave in pre-stressed thin elastomers" *Wave Motion* Vol. 43, 20-8, 2005.
- [6] Hallquist, J. O., *LS-DYNA Theoretical Manual*, LSTC, Livermore, CA, 1998.